# Emperical Model of the Microwave Properties of High-Temperature Superconductors

Orest G. Vendik, *Member, IEEE*, Irina B. Vendik, *Member, IEEE*, and Dimitri I. Kaparkov

***Abstract*— This paper presents simple correct models of high-temperature superconductor (HTS) film parameters at microwave frequencies. The models are based on the enhanced two-fluid model of a superconductor. The quasi-particle scattering and peculiarities of the normal conductivity of the HTS at microwaves, including residual resistance of a material, are taken into account. The difference between the known Gorter and Casimir two-fluid model of low-temperature superconductor and the enhanced two-fluid model of HTS is proven. A simple quasi-static model of current distribution across the microstrip line and coplanar waveguide is used for a simulation of a contribution of the superconductor transport processes into impedance per unit length of the transmission lines considered. The models developed were applied to a simulation of microstrip line and coplanar waveguide resonators. Good agreement of simulated results and measurements in a wide temperature range has been demonstrated. The model presented can be considered as a starting point for the formation of the computer-aided design (CAD) package of HTS microwave components.**

***Index Terms*— High-temperature superconductors, modeling, superconducting films, superconducting transmission lines, surface impedance.**

## I. Introduction

MODELING surface impedance of high-temperature ($T_c$) superconductors (HTS's) is an important component of a computer-aided design (CAD) of microwave devices which are intended for use at the liquid nitrogen temperature. Many attempts to find an adequate description of the surface impedance of the high-$T_c$ superconductors as a function of temperature and frequency are known [1]–[12]. The problem is complicated by the absence of an accomplished theory of the high-$T_c$ superconductivity. Engineers are faced with the necessity to describe a phenomenon in the situation when the nature of the phenomenon has not been theoretically explained. A description that is quantitatively adequate to the macroscopic properties of the phenomenon, but not using its microscopic nature, is referred to as a phenomenological model. There are many known phenomenological models of phenomena used in electronics and electrical engineering. Such models successfully serve in the cases when there is no theoretical model of the phenomenon or the rigid theory of it is very complicated to be understand and used. The goal of this paper is to formulate the requirements to the phenomenological description and to select the most favorable phenomenological description of the high-$T_c$ superconductors.

Manuscript received July 31, 1996; revised February 13, 1998. This work was supported by the Royal Swedish Academy of Sciences, by the National Board for Industrial and Technical Development in Sweden, and by the Science Council on Condensed Matter under Project 98063 in Russia.

O. G. Vendik is with the Department of Electronics, St. Petersburg Electrotechnical University, St. Petersburg, Russia 197376.

I. B. Vendik is with the Department of Microelectronics and Radio Engineering, St. Petersburg Electrotechnical University, St. Petersburg, Russia 197376.

D. I. Kaparkov is with the Microwave Research Group, Department of Microelectronics, St. Petersburg Electrotechnical University, St. Petersburg, Russia 197376.

Publisher Item Identifier S 0018-9480(98)03161-5.

## II. Requirements to Model Description Based on a Phenomenological Theory

A phenomenological theory can be used as a basis of an empirical model of the phenomenon. The following requirements to the model can be formulated:

1) model is founded on simple physical ideas;
2) model is in a reasonable agreement with known experimental data;
3) model comprises simple and correct formulas;
4) within specified limits of the variables employed, the model obeys the laws of the fundamental physics;
5) model can be easily inserted into CAD systems which are in common use.

As a brilliant example of a phenomenological approach to the nature of superconductivity, the Gorter and Casimir two-fluid model of a superconductor can be considered. The Gorter and Casimir two-fluid model was suggested in 1934 when the rigorous theory of superconductivity had not yet been contemplated.

The principal idea of the two-fluid model consists of the description of the electron subsystem of a superconductor in a form of two noninteracting fluids: the superconducting fluid (S-fluid) formed by the charge carriers in the superconducting state and the normal fluid (N-fluid) formed by the charge carriers in the normal state. It is worth mentioning that the charge carriers in the normal state are often called quasi-particle excitations as well.

## III. Two-Fluid Model of a Superconductor

The starting point of the two-fluid model is a suggestion about temperature dependence of densities of the charge carriers in the S- and N-states. The simplest form of these dependencies is given by the following empirical relations:

$$n_s(T) = n_0 \begin{cases} 0, & \text{for } T \geq T_c \\ 1 - (T/T_c)^{\gamma}, & \text{for } T \leq T_c \end{cases}$$
$$n_n(T) = n_0 \begin{cases} 1, & \text{for } T \geq T_c \\ (T/T_c)^{\gamma}, & \text{for } T \leq T_c \end{cases} \quad (1)$$

where $T$ is the temperature, $T_c$ is the critical temperature, $n_0$ is the total electron density in the superconductor, and $\gamma$ is an exponent.

For conventional superconductors such as Pb, Sn, and Nb which were known in the time when the Gorter and Casimir model had been suggested, a good agreement with the experiment was provided by $\gamma = 4$. The value of the exponent $\gamma$ for the high-$T_c$ superconductors will be discussed later.

The $n_s(T)$ is closely connected with the principal parameter of a superconductor $\lambda_L(T)$—the penetration depth of a magnetic field, so-called London penetration depth [13]

$$\frac{1}{\lambda_L(T)^2} = \frac{e^2 n_s(T)\mu_0}{m_s} \tag{2}$$

where $e$ and $m_s$ are charge and effective mass of an electron, and $\mu_0$ is the free-space magnetic permittivity.

The London penetration depth can be measured experimentally. The measurement of $\lambda_L(T)$is a way to find the experimental dependence of $n_s(T)$. That is why Section IV of this paper is dedicated to the London penetration depth as a function of temperature.

## IV. London Penetration Depth as a Function of Temperature

The dependence of the penetration depth $\lambda_L(T)$ of a magnetic field in high-$T_c$ superconductors has been studied experimentally in many investigations [14]–[22]. These dependencies are generally approximated in the binomial form

$$[\lambda_L(0)/\lambda_L(T)]^2 = 1 - (T/T_c)^\gamma \tag{3}$$

where $\lambda_L(0)$is the penetration depth for $T \to 0$.

The simplest theoretical model of the high-$T_c$ superconductors utilizing the idea of localized bosons (bipolarons) undergoing Bose–Einstein condensation [23], [24] yields $\gamma = 1.5$. However this model is a rough approximation and is best regarded as a phenomenological description that is convenient in some cases for quantitative estimates [1]–[4]. More rigorous study of the nature of high-$T_c$ superconductors yields a dependence of $\lambda_L(T)$ similar to that given by the Bardeen–Cooper–Schrieffer (BCS) theory. However most theoretical studies based on a concept of gap features in high-$T_c$ superconducting materials—two gaps [19], gaps with nods [25], gapless model [26]—or on the inhomogeneity or multiphase nature of the composition of high-$T_c$ superconductors [19], [27], [28], arrive at the idea of description of the dependence $\lambda_L(T)$ in the form (3).

It is worth discussing here the determination of the parameters $\gamma$, $\lambda_L(0)$, and $T_c$ in [5] based on the experimental data [14]–[18]. The experimental data were presented by the set of pairs of numbers $\lambda_i$ and $T_i$. The sum of the squares of the differences between the values of $\lambda_i$ measured at a temperature $T_i$ and those calculated using (1) was compiled as follows:

$$S[\lambda_L(0), T_c, \gamma] = \sum_{i=1}^{N} \{[\lambda_L(0)/\lambda_i]^2 - [1-(T/T_c)^\gamma]\}^2 \tag{4}$$

where $N$ is the number of experimental points. The set of parameters $\gamma$, $\lambda_L(0)$, and $T_c$ is determined from the condition of minimum $S$. The reliability of the approximation was estimated using the following sum:

$$\delta = \frac{1}{\lambda_L(0)} \sqrt{\frac{1}{N}\sum_{i=1}^{N}\left[\lambda_i - \frac{\lambda_L(0)}{\sqrt{1-(T_i/T_c)^\gamma}}\right]^2}. \tag{5}$$

TABLE I
Characteristics of YBCO Films Based on Experimental Data [14]–[18]

| $\lambda_L(0)$, nm | $T_c$, K | $\gamma$ | $\delta$ | References |
|---|---|---|---|---|
| 134.8 | 89.4 | 2.05 | 0.04 | [14] |
| 219.0 | 88.5 | 1.68 | 0.06 | [15] |
| 261.7 | 69 | 1.45 | 0.35 | [16] |
| 147.7 | 91.4 | 2.08 | 0.30 | [17] |
| 144.7 | 93.0 | 2.00 | 0.10 | [18] |

As a test for the proposed procedure, the algorithm described was applied to a traditional low-temperature superconductor—lead—experimental data being taken from [29]. The following parameters were obtained: $T_c = 7.198$ K, $\lambda_L(0) = 48.1$ nm, $\gamma = 4.204$, $\delta = 0.06$ which are in a very good agreement with the commonly used Gorter–Casimir presentation for the traditional low-temperature superconductors. That approves the reliability of the algorithm described.

The results of an analysis of the experimental results on $\lambda_L(T)$ for a Y–Ba–Cu–O superconductor are presented in Table I.

The data of Table I are in agreement with [20], where the best fit of experimental data and the relation (3) based on least-square estimation yields $\gamma = 1.7$ and $\lambda_L(0) = 156$ nm.

The Y–Ba–Cu–O films studied experimentally may be classified into two groups: high-quality films $\lambda_L(0) \leq 150$ nm, $T_c \geq 89$ K and low-quality films $\lambda_L(0) > 150$ nm, $T_c < 89$ K.

The classification of the films according to their quality agrees with the usual estimates. On the basis of the data presented in Table I, it may be concluded that a phenomenological description of $\lambda_L(T)$ for the high-quality Y–Ba–Cu–O films may be achieved for $\gamma = 2.0$. For the low-quality films, $\gamma = 1.5$ is more accurate. Among some experimental results, one may find $\gamma = 1.3$–$1.4$. The smoother dependence of $\lambda_L(T)$ for low-quality films may be attributed to broadening of the phase transition caused by inhomogeneity of the phase composition of the films.

Thus, the Gorter–Casimir relations (1) can be applied both to the low-temperature superconductors with $\gamma = 4.0$, and to the HTS's with $\gamma = 1.3$–$2.1$. The two-fluid model as applied to HTS's is called the "enhanced" or "modified" two-fluid model [10], [30]–[34].

The dependence of $\lambda_L(T)$ for different values of $\lambda_L(0)$ and $\gamma$ is presented in Table II, and may be used as a guide for orientation with actual values of the London penetration depth at the different temperatures.

The row $T = 78$ K corresponds to the liquid-nitrogen temperature.

TABLE II
LONDON PENETRATION DEPTH FOR $YBa_2Cu_3O_7$ ($T_c = 90$ K)

| $\lambda_n(0)$ | 150 nm | | 200 nm | | 250 nm | |
|---|---|---|---|---|---|---|
| T, K | $\gamma = 1.5$ | $\gamma = 2.0$ | $\gamma = 1.5$ | $\gamma = 2.0$ | $\gamma = 1.5$ | $\gamma = 2.0$ |
| 4.2 | 151 | 150 | 201 | 200 | 251 | 250 |
| 30 | 167 | 159 | 223 | 212 | 278 | 265 |
| 60 | 222 | 201 | 296 | 268 | 370 | 335 |
| **78** | **341** | **301** | **455** | **401** | **569** | **501** |
| 85 | 523 | 456 | 698 | 609 | 872 | 761 |
| 89 | 1164 | 1009 | 1551 | 1345 | 1939 | 1682 |

## V. QUASI-PARTICLE SCATTERING AND NORMAL CONDUCTIVITY OF HIGH-$T_c$ SUPERCONDUCTOR

Quasi-particles (normal electrons) do not take part in a response of a superconductor on the $dc$ electric field because the $dc$ electric field equals zero inside of the superconducting body. The microwave electric field penetrates inward a superconductor and initiates a motion of the quasi-particles. In two-fluid approach, the qausi-particles are presented by the N-state fluid. The response of the N-state fluid is characterized by the normal conductivity of the material as follows:

$$\sigma_n(T) = \frac{e^2 n_n(T)}{m_n} \cdot \tau(T) \tag{6}$$

where $\tau(T)$ is the quasi-particle relaxation time, other notations were introduced before.

We suppose that the effective mass of the normal electrons is constant and does not depend on temperature. The specific feature of the HTS is that the normal conductivity of the HTS is inversely proportional to the temperature at $T > T_c$. The simple explanation of such a dependence of $\sigma_n(T)$ on $T$ was done by Mott [24]. The dependence of $\sigma_n(T)$ on $T$ at $T > T_c$ is supported by the experimental results. The dependence of $\sigma_n(T)$ on $T$ is determined by $n_n(T)$ and $\tau(T)$. An appropriate treatment [20] of the experimental data yields the numerical results presented in Fig. 1. The following empirical formula is suggested to fit the experimental data

$$\frac{1}{\tau(t)} = \frac{1}{\tau(1)} \cdot \begin{cases} t, & t \geq 1 \\ \dfrac{t}{1 + \alpha(t^{1-\gamma} - t)}, & t \leq 1 \end{cases} \tag{7}$$

where $t$ is the reduced temperature

$$t = \frac{T}{T_c} \tag{8}$$

and $\alpha$ is an empirical parameter.

Fig. 1 illustrates (7) with $\tau(1) = 3.57 \cdot 10^{-14}$ s, $\alpha = 10$, and $\gamma = 1.5$.

Substituting $n_n(T)$ from (1) and $\tau(T)$ from (7) into (6) yields

$$\sigma_n(t) = \sigma_n(1) \begin{cases} t^{-1}, & \text{for } t \geq 1 \\ t^{\gamma-1} + \alpha \cdot (1 - t^{\gamma}), & \text{for } t \leq 1. \end{cases} \tag{9}$$

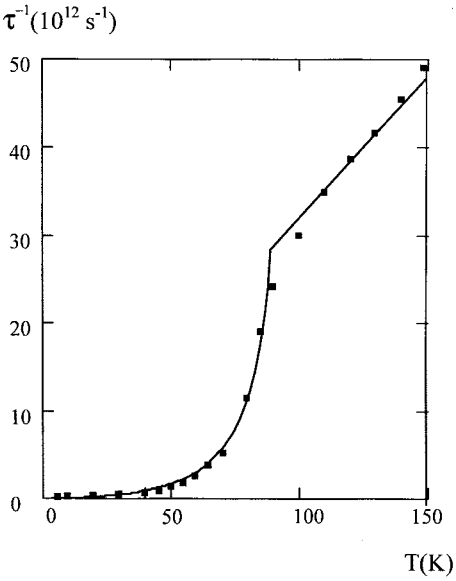


Fig. 1. The temperature dependence of the relaxation time $\tau(t)$ in comparison with the experimental results [20]. The model parameters $\tau(1) = 3.57 \cdot 10^{-14}$ s, $\gamma = 1.5$, and $\alpha = 10$ are used.

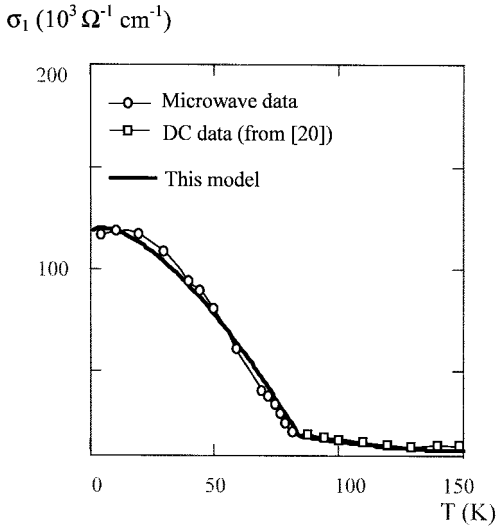


Fig. 2. The temperature dependence of the normal conductivity $\sigma_n(t)$ in comparison with the experimental results [20]. The model parameters $\sigma_n(1) = 1.8 \cdot 10^6$ $(\Omega \cdot \mathrm{m})^{-1}$, $\gamma = 1.5$, and $\alpha = 6.5$ are used.

Fig. 2 shows (9) in comparison with the experimental results [20].

In a perfect superconductor, the normal electron density must be zero at the limit $T \to 0$ K. But in the real situation, $n_n(0) \neq 0$. The presence of nonpairing charge carriers at $T \to 0$ K results in so-called residual resistance that characterizes the properties of a superconductor at very low temperature. The principal role of nonpairing charge carriers at $T \to 0$ K in HTS was suggested by Müller *et al.* [35] and used in "three-fluid model" by Kobayashi [6]–[9]. The contribution of the "third" fluid into HTS response to the microwave field was discussed later [4]. It was suggested that the nonpairing charge carriers in HTS are situated in the O–Cu–O chains in the Y–Ba–Cu–O crystal structure.

At the temperature range $0.5T_c < T < T_c$, the contribution of the "third" fluid in the high-temperature superconductor chain response to the microwave field is covered numerically by peculiarities of the temperature dependence of the quasi-particle relaxation time. One can see that the empirical formula (9) introduced in this section gives

$$\text{for } T = T_c, \qquad \sigma_n(T_c) = \sigma_n(1)$$
$$\text{for } T \to 0\,\text{K}, \qquad \sigma_n(0) = \alpha \cdot \sigma_n(1).$$

This enables one to say that the parameter $\alpha$ is responsible for the residual resistance of a superconductor.

## VI. Electrodynamics of High-$T_C$ Superconductor

The Maxwell equations are the foundation of consideration throughout this section:

$$\begin{aligned} \text{curl}\vec{\text{E}} &= -i\omega\mu_0 \vec{H} \\ \text{curl}\vec{\text{H}} &= i\omega\varepsilon_0 \vec{E} + \vec{j_s} + \vec{j_n} \end{aligned} \tag{10}$$

where $\vec{j_s}$ and $\vec{j_n}$ are super- and normal-current densities.

Let us use the well-known kinetic formulas for the super- and normal-current densities

$$\begin{aligned} \vec{j_s} &= en_s\vec{v}_s \\ \vec{j_n} &= en_n\vec{v}_n \end{aligned} \tag{11}$$

where $\vec{v}_s$ and $\vec{v}_n$ are the drift velocities of the charge carriers in the S- and N-states, respectively.

It is necessary to stress that the kinetic formulas (11) are correct in the case when

$$\begin{aligned} \frac{\partial n_s}{\partial t} &= 0, \qquad \text{grad } n_s = 0 \\ \frac{\partial n_n}{\partial t} &= 0, \qquad \text{grad } n_n = 0 \end{aligned} \tag{12}$$

otherwise the current arising from the change in time of the accumulated charge and the current associated with the diffusion of the charge carriers should be included in (11).[1]

The following Newton equation of motion is used:

$$\begin{aligned} m_s\frac{d\vec{v}_s}{dt} &= e\vec{E} \\ m_n\frac{d\vec{v}_n}{dt} + m_n\frac{\vec{v}_n}{\tau} &= e\vec{E} \end{aligned} \tag{13}$$

where $\tau$ is the quasi-particle relaxation time.

Taking into account that the period of microwave oscillations is much higher than the quasi-particle relaxation time in the temperature range $0.5T_c < T < T_c$ (see Fig. 1), the term with $d\vec{v}_n/dt$ may be cancelled.

Thus, combining (11) and (13), one obtains

$$\begin{aligned} \vec{j_s} &= \frac{1}{\lambda_L^2} \cdot \frac{1}{i\omega\mu_0}\vec{E} \\ \vec{j_n} &= \sigma_n\vec{E}. \end{aligned} \tag{14}$$

[1] We must note that in [11] and [12] where the authors use supposition, that the derivative of $n_s$ with respect to time is not zero. The results obtained in [11] and [12] seem quite reasonable as a pnenomenological description of a superconductor at microwaves. But from the science–logic point of view, we must say that they disobey the principles of the solid-state physics and cannot be accepted.

Substituting (14) into the Maxwell equations yields the following equations with the effective dielectric constant:

$$\varepsilon = \begin{cases} -i\dfrac{\sigma_n}{\omega}, & \text{for } T \geq T_c \\ -i\dfrac{\sigma_n}{\omega} - \dfrac{1}{\omega^2\lambda_L^2\mu_0}, & \text{for } T \leq T_c. \end{cases} \tag{15}$$

Here, the inequality $\varepsilon_0 \ll \sigma_n/\omega$ is taken into account.

The wavenumber $k$ and the wave impedance $Z_0$ for the wave propagating in the superconducting medium can be found. Doing this, we may replace $\varepsilon_0$ by $\varepsilon$ in the known expressions $k = \omega\sqrt{\varepsilon_0\mu_0}$, $Z_0 = \sqrt{\mu_0/\varepsilon_0}$. Thus

$$k = \begin{cases} (1-i)\sqrt{\dfrac{\omega\mu_0\sigma_n}{2}}, & \text{for } T \geq T_c \\ \sqrt{-i\omega\mu_0\sigma_n - \dfrac{1}{\lambda_L^2}}, & \text{for } T \leq T_c \end{cases} \tag{16}$$

$$Z_0 = \begin{cases} (1+i)\sqrt{\dfrac{\omega\mu_0}{2\sigma_n}}, & \text{for } T \geq T_c \\ \dfrac{i\omega\mu_0}{\sqrt{1+i\omega\mu_0\sigma_n\lambda_L^2}}, & \text{for } T \leq T_c. \end{cases} \tag{17}$$

## VII. Surface Impedance of Bulk or Thin-Film Superconducting Sample

For a plane electromagnetic wave incident normally on the sample surface, the ratio of $|\boldsymbol{E}|$ to $|\boldsymbol{H}|$ taken on the surface of the sample is called the surface impedance. If the thickness of the sample in the direction of the wave propagation is comparable with the London penetration depth, the interference of the waves reflected from both sides of the sample should be taken into account. If the back side of the sample is open and the wave impedance of the superconducting medium is extremely small in comparison with the wave impedance of the vacuum, the surface impedance of the sample is

$$Z_{\text{sur}} = R_{\text{sur}} + iX_{\text{sur}} = \frac{Z_0}{\tanh(ikd)} \tag{18}$$

where $Z_0$ and $k$ are determined by the expressions (16) and (17).

The surface resistance $R_{\text{sur}}$ and surface reactance $X_{\text{sur}}$ can be found using (16)–(18), dealing with the complex variables considering as functions of temperature. In order to simplify the calculation and to clarify the results, the series expansion can be used. After some transformations, one obtains for $T < T_c$

$$R_{\text{sur}}(T) = \begin{cases} \frac{1}{2}(\omega\mu_0)^2\lambda_L^3(T)\sigma_n(T), & \text{for } d \geq 2\lambda_L \text{ (bulk sample)} \\ (\omega\mu_0)^2\dfrac{\lambda_L^4(T)}{d}\sigma_n(T), & \text{for } d \leq 2\lambda_L \text{ (thin film)} \end{cases} \tag{19}$$

and

$$X_{\text{sur}}(T) = \begin{cases} \omega\mu_0\lambda_L(T), & \text{for } d \geq 2\lambda_L \text{ (bulk sample)} \\ \omega\mu_0\dfrac{\lambda_L^2(T)}{d}, & \text{for } d \leq 2\lambda_L \text{ (thin film).} \end{cases} \tag{20}$$

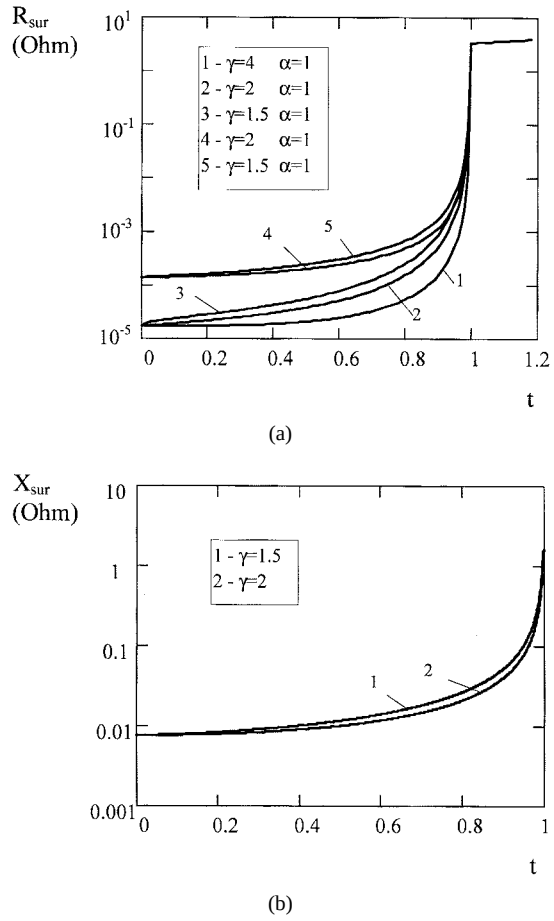


Fig. 3. The temperature dependence of the (a) real and (b) imaginary parts of the surface impedance for different model parameters $\alpha$ and $\gamma$ calculated for $\sigma_n(1) = 10^6\ (\Omega\cdot\mathrm{m})^{-1}$, $\lambda_L(0) = 0.17\,\mu$m, $d = 0.3\ \mu$m, and $f = 10$ GHz.

Given formulas yield the correct numerical results for $d \leq \lambda_L$ or for $d \geq 3\lambda_L$. The maximum error takes place at the point $d = 2\lambda_L$ and reaches there $\approx 9\%$.

Formulas (19) and (20) cannot be used in the point $T = T_c$ where the binomial (3) gives $\lambda_L \to \infty$. For crossing the point $T = T_c$, (21) and (22), shown at the bottom of the page, could be suggested (in the case $d < 2\lambda_L$).

Fig. 3 illustrates the dependencies given by (21) and (22).

Thus, the empirical (phenomenological) model of the microwave properties of an HTS sample is developed. In order to provide a correct description of the microwave properties of an HTS sample, five fitting parameters are used. The parameters and their reasonable values for $YBa_2Cu_3O_7$ are presented in Table III.

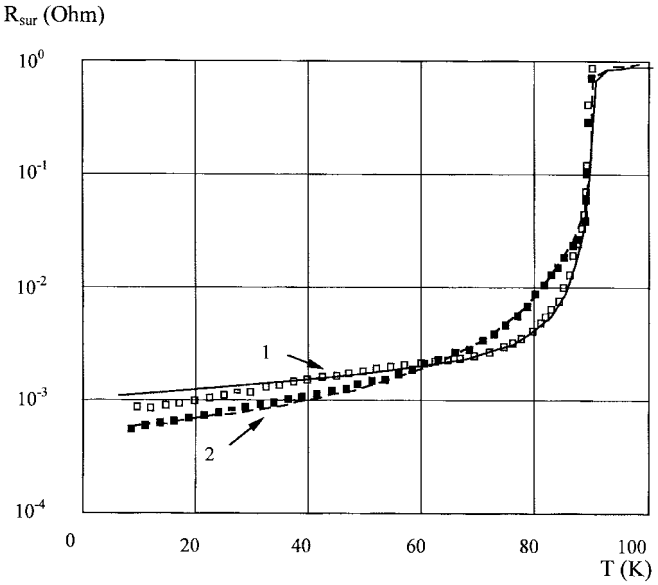


Fig. 4. Modeling surface resistance of HTS films at $f = 19$ GHz in accordance with the experimental data [37]. Curve 1: $T_c = 90$ K, $d = 0.3\ \mu$m, $\sigma_n(1) = 4.3\cdot 10^6\ (\Omega\cdot\mathrm{m})^{-1}$, $\lambda_L(0) = 0.17\ \mu$m, $\gamma = 2$, and $\alpha = 3.5$. Curve 2: $T_c = 90$ K, $d = 0.3\ \mu$m, $\sigma_n(1) = 4.3\cdot 10^6\ (\Omega\cdot\mathrm{m})^{-1}$, $\lambda_L(0) = 0.17\ \mu$m, $\gamma = 1.5$, and $\alpha = 2.5$.

TABLE III
TYPICAL PHENOMENOLOGICAL PARAMETERS OF YBCO FILMS

| No | Parameter | Notation | Range of values |
|---|---|---|---|
| 1 | Critical temperature | $T_c$ | 88 - 92 K |
| 2 | Exponent | $\gamma$ | 1.3 - 2.3 |
| 3 | Penetration depth at 0 K | $\lambda_L(0)$ | 120 - 260 nm |
| 4 | Conductivity at T = $T_c$ | $\sigma_n(1)$ | $(1 - 3)\cdot 10^6$ 1/Ω•m |
| 5 | Residual resistance rate | $\alpha$ | 1 -20 |

A set of experimental data for the surface resistance of the HTS films was processed, with the results demonstrating a good agreement between measured and simulated data [36]. Here, we use the experimental data for surface resistance of the HTS films obtained by Klein *et al.* [37]. Fig. 4 demonstrates good agreement between measured and simulated data; the fitting parameters are given in the legend to the picture. Curve 1 corresponds to the measurement of the sample which was kept after growing for a period of four days at room temperature in dry air. The set of model parameters for this

$$R_{\mathrm{sur}}(T) = \begin{cases} \dfrac{1}{\sigma_n(T)d}, & \text{for } T \geq T_c \text{ (N-state)} \\ \dfrac{(\omega\mu_0)^2\sigma_n(T)}{1+[\omega\mu_0\sigma_n(T)\lambda_L^2(T)]^2}\cdot\dfrac{\lambda_L^4(T)}{d}, & \text{for } T \leq T_c \text{ (S-state)} \end{cases} \tag{21}$$

$$X_{\mathrm{sur}}(T) = \begin{cases} 0, & \text{for } T \geq T_c \text{ (N-state)} \\ \dfrac{\omega\mu_0}{1+[\omega\mu_0\sigma_n(T)\lambda_L^2(T)]^2}\cdot\dfrac{\lambda_L^2(T)}{d}, & \text{for } T \leq T_c \text{ (S-state)} \end{cases} \tag{22}$$

characteristics is used: $T_c = 90$ K, $d = 0.3$ $\mu$m, $\sigma_N(1) = 4.3 \cdot 10^6\,(\Omega \cdot \mathrm{m})^{-1}$, $\lambda_L(0) = 0.17$ $\mu$m, $\gamma = 2$, $\alpha = 3.5$. Curve 2 was measured for the same sample postannealed at 200°C in molecular oxygen and then slowly cooled down. After annealing, the residual resistance decreased, though the surface resistance near $T_c$ became higher. This behavior is described by corresponding change of the model parameters $\gamma = 1.5$ and $\alpha = 2.5$.

The model uses $f^2$ dependence of $R_{\mathrm{sur}}$ on frequency, which is in a good agreement with the experiment and the theory [13], [38], [39] and can be actually observed in the case of good quality samples. If the samples contain some normally conducting inclusions or intergranular Josephson-like weak links, the frequency dependence of $R_{\mathrm{sur}}$ becomes weaker than $f^2$ and should be specially described by suitable models (e.g., [11], [12]). This problem lays out of the scope of this paper.

## VIII. Propagation Parameters of Microstrip and Coplanar Lines Based on the HTS Films

Propagation parameters of a transmission line are the phase velocity and the attenuation coefficient. The phase velocity is determined by the inductance and the capacitance per unit length of the line

$$v_{ph} = \frac{1}{\sqrt{L_1 C_1}} \tag{23}$$

and is often presented in the form

$$v_{ph} = \frac{c}{\sqrt{\varepsilon_{\mathrm{eff}}}} \tag{24}$$

where $c$ is the light velocity in the free space, and $\varepsilon_{\mathrm{eff}}$ is the effective dielectric constant of the line.

In the case of a superconducting transmission line, the total inductance per unit length is the sum of the geometric inductance $L_1^g$ and the kinetic inductance $L_1^k$:

$$L_1 = L_1^g + L_1^k. \tag{25}$$

The geometric inductance related to the external magnetic field is determined by the geometry of the line. The kinetic inductance is determined by the transport properties of the charge carriers in the superconducting parts of the line and depends sufficiently on a nonhomogeneity of a surface current density distribution across the conductor.

Comparing (23)–(25), one can find the effective dielectric constant of the superconducting transmission line as

$$\varepsilon_{\mathrm{eff}} = \varepsilon_{\mathrm{eff}}^0 \left(1 + \frac{L_1^k}{L_1^g}\right). \tag{26}$$

The effective dielectric constant $\varepsilon_{\mathrm{eff}}^0$ for a microstrip line or a coplanar waveguide can be calculated with essential accuracy using known expressions published elsewhere. The surface kinetic inductance can be found from (22) while presenting

$$X_{\mathrm{sur}}(T) = \omega L^k(T). \tag{27}$$

The attenuation in a transmission line caused by loss in conductors is determined by the known expression

$$\alpha = \frac{R_1}{2Z_0} \tag{28}$$

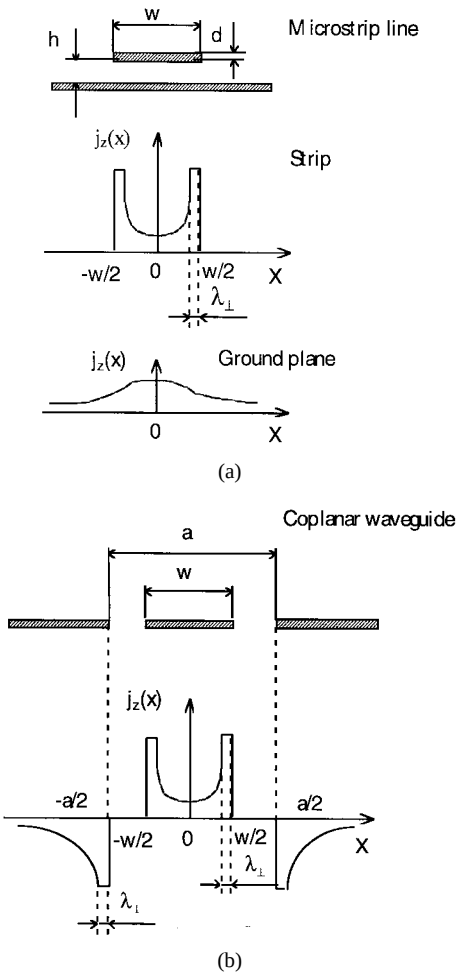


Fig. 5. Surface current density distribution in the conductors of (a) HTS microstrip line and (b) HTS coplanar waveguide.

where $R_1$ is the resistance per unit length and

$$Z_0 = \sqrt{\frac{L_1^g + L_1^k}{C_1}} \tag{29}$$

is the wave impedance of the line.

The real and imaginary parts of the line impedance per unit length depend on the surface current density distribution across the conductor of the line. Fig. 5 illustrates the current distribution in the conductors of the microstrip line and the coplanar waveguide. The surface current density distribution in superconducting transmission lines was widely investigated and modeled [40]–[42]. We use the magnetostatic approach in order to obtain simple analytical formulas describing current distribution across the microstrip line [43] and the coplanar waveguide [44]. It is suggested that the current density at the edges is homogeneous on the distance of $\lambda_\perp$, as illustrated by Fig. 5. The edge penetration depth $\lambda_\perp$[2] is related to the London penetration depth $\lambda_L$ as

$$\lambda_\perp = \frac{2\lambda_L^2(t)}{d}. \tag{30}$$

[2] In more general consideration, $\lambda_\perp$ was introduced as a penetration depth in a thin film around the magnetic vortex and is known as the Pearl's penetration depth [45].

This approach allows one to obtain simple and correct formulas for propagation parameters of the lines.

Taking into account the surface current density $j_z(x)$ [43], [44], one obtains the real and imaginary parts of the line impedance per unit length

$$R_1 = \frac{1}{|I|^2} R_{\text{sur}} \int_{-\infty}^{\infty} j_z^2(x)\, dx \tag{31}$$

$$X_1 = \frac{1}{|I|^2} X_{\text{sur}} \int_{-\infty}^{\infty} j_z^2(x)\, dx. \tag{32}$$

Here, $I$ is the total current which flows along the line.

### A. Microstrip Line

The resistance per unit length $R_1$ for an HTS microstrip line is determined by the strip surface resistance $R_{\text{sur}}^{\text{strip}}$ and the ground plane surface resistance $R_{\text{sur}}^{\text{g.p.}}$

$$R_1 = \frac{1}{|I|^2} R_{\text{sur}}^{\text{strip}} \int_{-w/2}^{w/2} j_{z,\,\text{strip}}^2(x)\, dx + \frac{1}{|I|^2} R_{\text{sur}}^{\text{g.p.}} \int_{-\infty}^{\infty} j_{z,\,\text{g.p.}}^2(x)\, dx \tag{33}$$

where $j_{z,\,\text{strip}}(x)$ and $j_{z,\,\text{g.p.}}(x)$ are the surface current distributions in the strip and the ground plane correspondingly. After integration, (33) can be presented as

$$R_1 = R_{\text{sur}}^{\text{strip}}/w_{\text{eff}} + R_{\text{sur}}^{\text{g.p.}}/h_{\text{eff}} \tag{34}$$

where

$$1/w_{\text{eff}} = (1/w)\cdot(8/\pi^2)\cdot[1 + 0.25\ln(w/\lambda_\perp - 1)] \tag{35}$$

$$1/h_{\text{eff}} = (1/h)\cdot\tanh(3h/2w). \tag{36}$$

The reactance per unit length for the HTS microstrip line in accordance with (27) and (32) is

$$X_1 = \omega L^k/w_{\text{eff}}. \tag{37}$$

Here, we neglect the contribution from the ground plane.

Expression (37) is followed by the kinetic reactance per unit length

$$L_1^k = \frac{\mu_0}{1 + [\omega\,\mu_0\sigma_n(T)\lambda_L^2(T)]^2} \cdot \frac{\lambda_L^2(T)}{d} \cdot \frac{1}{w_{\text{eff}}}. \tag{38}$$

Using (26) and (38), one can obtain the expression for the effective dielectric constant

$$\varepsilon_{\text{eff}} = \varepsilon_{\text{eff}}^0(1 + \Delta\varepsilon_{\text{eff}}^k) \tag{39}$$

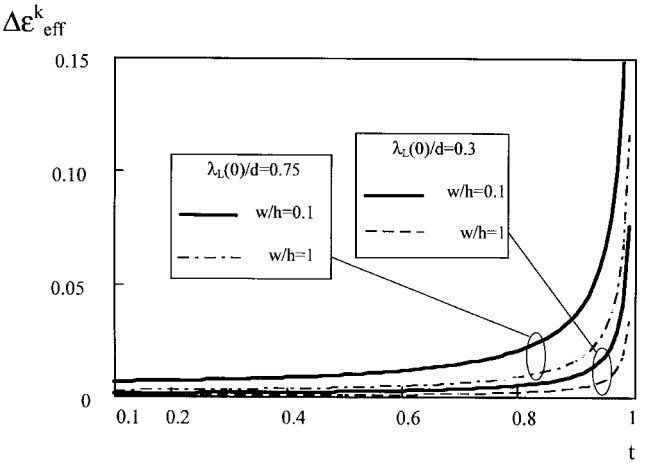


Fig. 6. The contribution of the kinetic inductance into the effective dielectric constant versus temperature ($\lambda_L(0) = 0.15\mu$m, $\gamma = 1.5$).

where

$$\Delta\varepsilon_{\text{eff}}^k = \frac{60\pi}{Z_0\sqrt{\varepsilon_{\text{eff}}^0}} \cdot \frac{\lambda_\perp}{w_{\text{eff}}}. \tag{40}$$

Influence of the kinetic inductance is noticeable at temperature $T > 0.8T_c$ and it is more pronounced for narrow lines, which is illustrated in Fig. 6.

### B. Coplanar Waveguide

The resistance per unit length for the HTS coplanar waveguide can be presented as a sum of the resistances of the central conductor $R_{1,1}$ and of the ground plane $R_{1,2}$ as follows:

$$R_1 = R_{1,1} + R_{1,2} = R_{\text{sur}} \cdot \frac{1}{w_{\text{eff}}} \tag{41}$$

where

$$\frac{1}{w_{\text{eff}}} = \frac{1}{w}(C_1 + C_2) \tag{42}$$

$$C_1 = \frac{2}{\left[K\left(\frac{w}{a}\right)\right]^2} \cdot \frac{1}{1 - \left(\frac{w}{a}\right)^2} \left[1 + \frac{1}{4}\ln\left(\frac{w}{\lambda_\perp} - 1\right) - \frac{w}{4a}\ln\left(\frac{a + w - 2\lambda_\perp}{a - w + 2\lambda_\perp}\right)\right] \tag{43}$$

$$C_2 = \frac{2}{\left[K\left(\frac{w}{a}\right)\right]^2} \cdot \frac{\frac{w}{a}}{1 - \left(\frac{w}{a}\right)^2} \left[1 + \frac{1}{4}\ln\left(\frac{a}{\lambda_\perp} + 1\right) - \frac{a}{4w}\ln\left(\frac{a + w - 2\lambda_\perp}{a - w + 2\lambda_\perp}\right)\right] \tag{44}$$

$K(w/a)$ is the complete elliptic integral of the first kind.

The kinetic inductance per unit length and the effective dielectric constant of the HTS coplanar waveguide are determined by (38) and (39) with $w_{\text{eff}}$ taken from (42).

The suggested model for propagation parameters of the HTS microstrip line and the HTS coplanar waveguide is valid while $\lambda_L$ is much less than the skin penetration depth, i.e.,

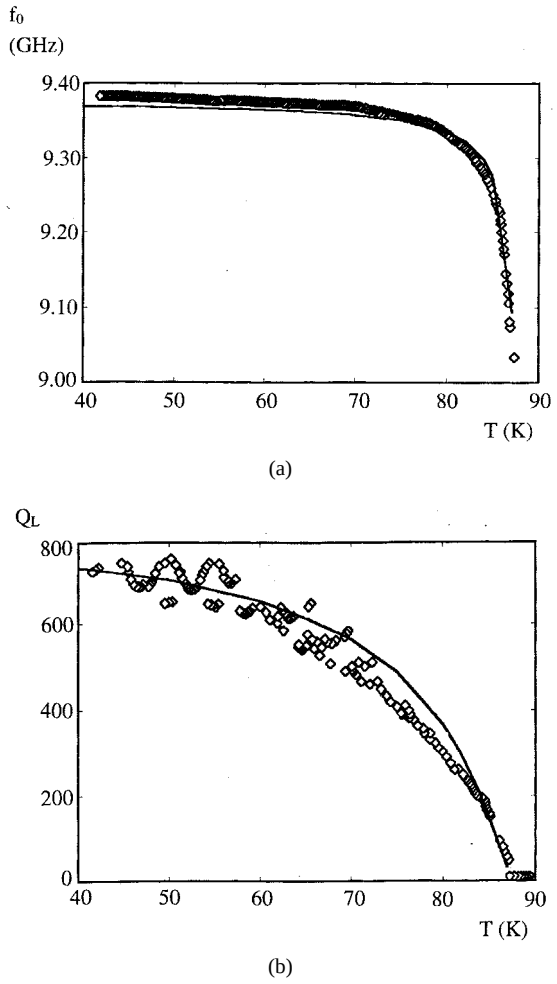


Fig. 7. Experimentally obtained and simulated dependencies of (a) resonant frequency and (b) loaded $Q$-factor on temperature for the HTS microstrip resonator. The model parameters $T_c = 88$ K, $d = 0.2$ $\mu$m, $\sigma_n(1) = 3 \cdot 10^6$ $(\Omega \cdot \mathrm{m})^{-1}$, $\lambda_L(0) = 0.16$ $\mu$m, $\gamma = 1.5$, and $\alpha = 20$ are used.

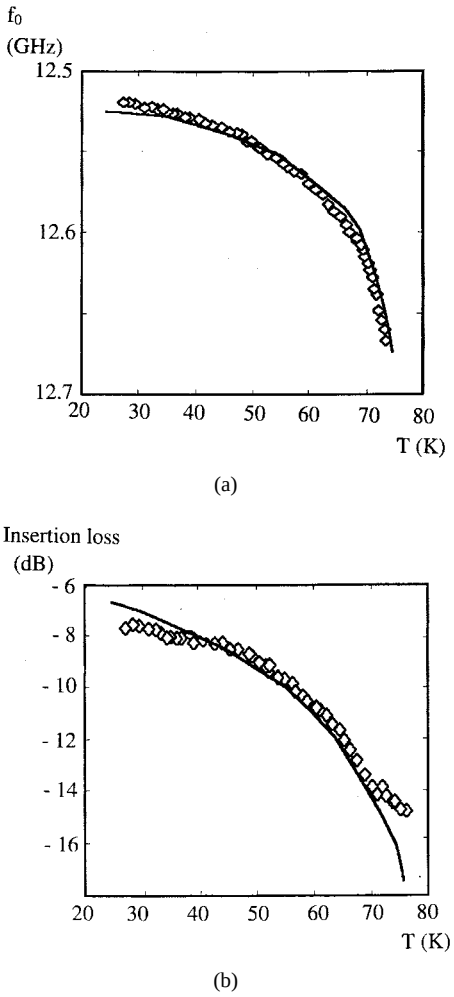


Fig. 8. Experimentally obtained and simulated dependencies of (a) resonant frequency and (b) insertion loss on temperature for the HTS coplanar waveguide The model parameters $T_c = 89.5$ K, $d = 0.35$ $\mu$m, $\sigma_n(1) = 2.6 \cdot 10^6$ $(\Omega \cdot \mathrm{m})^{-1}$, $\lambda_L(0) = 0.15$ $\mu$m, $\gamma = 1.3$, and $\alpha = 8$ are used. The dielectric constant of MgO at $T = 300$ K, $\varepsilon_r = 9.77$.

for high-$T_c$ superconductors, the approximation is suitable up to 100 GHz. The validity of the model was checked by comparison with the results of numerical calculations of the resistance per unit length for HTS microstrip line [41], [42] and coplanar waveguide [44], [46]. High accuracy of the model was exhibited in spite of the simplifications assumed.

## IX. Examples of Applications of the Model Developed

In practice, it is important to take into account specific microwave properties of HTS materials such as temperature behavior of penetration depth and a value of the residual resistance. A good illustration of this point is given by the temperature-dependent frequency response of resonators and filters. Resonator measurements are widely used for determination of the temperature dependence of the London penetration depth. In the majority of experiments, it was shown that this dependence differs from the two-fluid model suitable for low-temperature superconductors. Nevertheless, regarding full-wave analysis, the classical two-fluid model ($\gamma = 4$) can still be found in literature. Therefore, rigorous calculations based on physically incorrect models may give a significant discrepancy with experimental data, though mathematically they would seem to be correct.

For a simulation of characteristics of microstrip and coplanar resonators, we used the considered above model of the propagation parameters of the HTS transmission lines. The simulation makes use of $S$-parameters additionally taking into account the temperature dependence of copper conductivity, dielectric permittivity, and tangent of dielectric losses of substrate, and change of linear sizes of substrate due to cooling [47]. The results of simulation have been verified by measurements of the resonant characteristics in a wide temperature range. The experimental setup includes the Wiltron 360 B Network Analyzer and a closed-cycle cryocooler.

The microstrip resonator with YBCO film strip and copper ground plane was manufactured on a sapphire substrate. The resonator has 5.78-mm length, 0.5-mm width, and 0.352-mm coupling gaps. Fig. 7 shows the temperature dependence of the resonant frequency and the loaded $Q$ factor.

The simulation of the resonator takes into account anisotropic dielectric permittivity of sapphire [48], [49]. The accurate model of the coupling gap [50] is used.

The coplanar waveguide YBCO resonator on an MgO substrate have been also simulated and measured [51]. The resonator is 5-mm long, the width of the central conductor is 110 $\mu$m, the gaps are 50-$\mu$m wide. The coupling gaps are 0.5-mm long. We used an accurate model for the coupling gap [52]. The measured and simulated temperature dependencies of the resonant frequency and insertion loss of the HTS coplanar resonator are shown in Fig. 8.

As seen from Figs. 7(a) and 8(a), the use of the exponents $\gamma = 1.5$ (microstrip resonator) and $\gamma = 1.3$ (coplanar-waveguide resonator) in the model of the surface resistance of the HTS film allows one to obtain a precise dependence of the resonant frequency on temperature. A high accuracy of the model of the attenuation coefficient is collaborated by a good agreement between measured and simulated characteristics of the loaded $Q$ factor [Fig. 7(b)] and insertion loss at the resonant frequency [Fig. 8(b)] versus temperature.

## X. Conclusion

The simple and correct formulas have been developed for the surface impedance of HTS films at microwaves and the propagation characteristics of the HTS microstrip line and coplanar waveguide. The formulas can be considered as a starting point for a formation of a CAD package of HTS microwave components and devices. The first results in a development of the CAD of passive HTS microwave devices are already obtained [36], [53] and could be widely used.

## Acknowledgment

The authors are very grateful to E. Kollberg for numerous useful discussions and support.

## References

[1] O. G. Vendik, "Phenomenological model of a bipolaron superconductor," *Sov. Tech. Phys. Lett.*, vol. 14, pp. 482–483, June 1988.

[2] O. G. Vendik and A. Yu. Popov, "The critical current density of an oxide superconductor," *Phil. Mag. Lett.*, vol. 64, no. 3, pp. 143–145, 1991.

[3] ———, "Bipolaron theory approach to the microwave surface resistance of high-temperature superconductor," *Phil. Mag. Lett.*, vol. 65, no. 5, pp. 219–224, 1992.

[4] ———, "Can the bipolaron model be used for a description of microwave and infrared properties of a high-temperature superconductor?," *Philos. Mag. B, Phys. Condens. Matter Electron. Opt. Magn. Prop.* vol. 67, no. 6, pp. 833–845, 1993.

[5] O. G. Vendik, A. Yu. Popov, and S. P. Zubko, "Determination of the parameters of a phenomenological model of high-temperature superconductors," *Tech. Phys. Lett.*, vol. 21, pp. 585–586, Aug. 1995.

[6] Y. Kabayashi and T. Imai, "Phenomenological description of conduction mechanism of high-$T_c$ superconductors by three-fluid model," *IEICE Trans. Electron.*, vol. E74-C, pp. 1986–1992, July 1991.

[7] T. Imai, T. Sakakibara, and Y. Kobayashi, "Microwave characteristics of high-$T_c$ superconductors by improved three-fluid model," *IEICE Trans. Electron.*, vol. E76-C, pp. 1275–1279, Aug. 1993.

[8] Y. Kabayashi, T. Imai, and T. Sakakibara, "Phenomenological description of 'coherence peak' of high-$T_c$ superconductors by improved three-fluid model," in *Proc. 23rd European Microwave Conf.*, Madrid, Spain, Sept. 1993, pp. 596–599.

[9] T. Imai and Y. Kobayashi, "Phenomenological description of temperature and frequency dependence of surface resistance of high-$T_c$ superconductors by improved three-fluid model," *IEICE Trans. Electron.*, vol. E78-C, pp. 498–502, May 1995.

[10] D. S. Linden, T. P. Orlando, and W. G. Lyons, "Modified two-fluid model for superconductor surface impedance calculation," *IEEE Trans. Appl. Superconduct.*, vol. 4, pp. 136–141, Sept. 1994.

[11] J.-G. Ma and I. Wolf, "Modeling the microwave properties of superconductors," *IEEE Trans. Microwave Theory Tech.*, vol. 43, pp. 1053–1059, May 1995.

[12] ———, "Electromagnetic in high-$T_c$ superconductors," *IEEE Trans. Microwave Theory Tech.*, vol. 44, pp. 537–542, Apr. 1996.

[13] T. Van Duzer and C. W. Terner, *Principles of Superconductive Devices and Circuits.* Amsterdam, The Netherlands: Elsevier, 1981.

[14] J. M. Pond, K. R. Carrol, J. S. Horwitz, D. B. Chirsey, M. S. Osofsky, and V. S. Cestone, "Penetration depth and microwave loss measurement with a $YBa_2Cu3O_{7-\delta}/LaAlO_3/$ $YBa_2Cu3O_{7-\delta}$ trilayer transmission line," *Appl. Phys. Lett.*, vol. 59, pp. 3033–3036, Dec. 2, 1991.

[15] J. Y. Lee and T. R. Lemberger, "Penetration depth $\lambda(T)$ of $YBa_2Cu3O_{7-\delta}$ films determined from the kinetic inductance," *Appl. Phys. Lett.*, vol. 62, pp. 2419–2421, May 10, 1993.

[16] T. Kisu, T. Iinuma, K. Enpuku, K. Yoshida, and K. Yamafumi, "Magnetic penetration depth and critical current in YBaCuO thin films," *IEEE Trans. Appl. Superconduct.*, vol. 3, pp. 2961–2964, Mar. 1993.

[17] S. D. Brorson, R. Buhleier, J. O. White, L. E. Trofimov, H.-U. Habermeire, and J. Kuhl, "Kinetic inductance and penetration depth of thin superconducting films measured by THz-pulse spectroscopy," *Phys. Rev. B, Condens. Matter* vol. 49, pp. 6185–6187, Mar. 1993.

[18] D. A. Bonn, R. Liang, T. M. Risman *et al.*, "Microwave determination of the quasiparticle scattering time in $YBa_2Cu_3O_{6.95}$," *Phys. Rev. B, Condens. Matter* vol. 47, pp. 11314–11328, May 1993.

[19] N. Klein, N. Tellmann, H. Schulz, K. Urban, S. A. Wolf, and V. Z. Kresin, "Evidence of two-gap superconductivity in $YBa_2Cu_3O_{7-x}$ from microwave surface impedance measurements," *Phys. Rev. Lett.*, vol. 71, pp. 3355–3358, Nov. 15, 1993.

[20] F. Gao, J. W. Kruse, C. E. Platt, M. Feng, and M. V. Klein, "Microwave surface impedance at 10 GHz and quasiparticle scattering in $YBa_2Cu_3O_7$ films," *Appl. Phys. Lett.*, vol. 63, pp. 2274–2276, Oct. 1993.

[21] M. R. Beasly, "Recent penetration depth measurements of the high-$T_c$ superconductors and their implications," *Physica C*, vol. 209, pp. 43–46, Apr. 1993.

[22] U. Dähne, Y. Gorshunov, N. Klein, N. Tellmann, G. Kozlov, and K. Urban, "Frequency and temperature dependence of the millimeter wave conductivity of epitaxial $YBa_2Cu_3O_7$ films," *J. Superconductivity*, vol. 8, pp. 129– 134, Jan. 1995.

[23] A. S. Alexandrov, "Bipolarons of a small radius and anomalous properties of high temperature superconductors," *JEPT Lett.*, vol. 46, pp. S107–S109, June 1987.

[24] N. F. Mott "Electrical properties of oxide superconductors above $T_c$," *Philos. Mag. Lett.*, vol. 61, pp. 217–221, Feb. 1990.

[25] W. N. Hardy, D. B. Bonn, D. C. Morgan, R. Liang, and K. Zhang, "Precision measurements of the temperature dependence of $\lambda$ in $YBa_2Cu_3O_{6.95}$: Strong evidence for nodes in the gap function," *Phys. Rev. Lett.*, vol. 70, pp. 3999–4002, June 1993.

[26] V. A. Gasparov, M. R. Mktrchan, M. A. Obolensky, and A. V. Bondarenko, "Anomalous temperature dependence of the electromagnetic penetration depth of $YBa_2Cu_3O_{7-\delta}$ crystal," *Physica C*, vol. 231, pp. 196–206, Sept. 1994.

[27] A. L. Korzhenevskii and A. A. Luzhkov, "A phenomenological heterophase model of the conductivity anomalies in high-temperature superconductors," *Physica C*, vol. 204, pp. 191–193, Dec. 1992.

[28] O. G. Vendik, M. M. Gaidukov, S. G. Kolesov, A. B. Kozyrev, A. Y. Popov, and T. B. Samoilova, "Microwave properties of HTSC films as applied to microwave integrated circuit design," in *IV Bilateral Soviet–German Seminar High Temperature Superconductivity*, St. Petersburg, Russia, Oct. 1991, pp. 405–424.

[29] R. F. Gasparovic and W. L. McLean, "Superconducting penetration depth of lead," *Phys. Rev. B, Condens. Matter* vol. 2, pp. 2519–2526, Oct. 1970.

[30] O. R. Baiocchi, K.-S. Kong, and T. Itoh, "Pulse propagation in superconducting coplanar lines," *IEEE Trans. Microwave Theory Tech.*, vol. 40, pp. 509–511, Mar. 1992.

[31] F. Abbas and L. E. Davis, "Propagation coefficient in a superconducting asymmetrical parallel-plate transmission line with a buffer layer," *J. Appl. Phys.*, vol. 73, pp. 4494– 4499, May 1993.

[32] D. Ladret, B. Cabon, J. Chilo, P. Xavier, J. Richard, and O. Buisson, "Penetration depth extraction in high temperature superconducting microwave transmission lines," *J. Phys. (Paris) Colloque C6*, vol. 4, pp. C-211–C-216, June 1994.

[33] F. Abbas, L. E. Davis, and J. C. Gallop, "Ultra-high $Q$ resonators for low-noise microwave signal generation using sapphire buffer layers and

superconducting thin films," *Supercond. Sci. Tech.*, vol. 7, no. 7, pp. 495–501, July 1994.
[34] F. Abbas, "Propagation in a multilayer structure of superconductors and dielectrics," *Physica C*, vol. C254, pp. 291–306, Nov. 1995.
[35] G. Müller, N. Klein, A. Brust, H. Chaloupka, M. Hein, S. Orbach, H. Piel, and D. Reschke, "Survey of microwave surface impedance data of high-$T_c$ superconductors—Evidence for nonpairing charge carriers," *J. Superconductivity*, vol. 3, pp. 235–242, Mar. 1990.
[36] O. Vendik and E. Kollberg, "Software models HTSC microstrip and coplanar lines," *Microwaves RF*, vol. 32, pp. 118–121, July 1993.
[37] N. Klein, U. Poppe, N. Tellmann, H. Schulz, W. Evers, U. Dähne, and K. Urban, "Microwave surface resistance of epitaxial $YBa_2Cu_3O_{7-x}$ film: Studies on oxygen deficiency and disordering," *IEEE Trans. Appl. Superconduct.*, vol. 3, pp. 1102–1109, Mar. 1993.
[38] H. Piel and G. Müller, "The microwave surface impedance of high-$T_c$ superconductors," *IEEE Trans. Magn.*, vol. 27, pp. 854–862, Mar. 1991.
[39] Z.-Y. Shen, *High-Temperature Superconducting Microwave Circuits.* Norwood, MA: Artech House, 1994.
[40] D. M. Sheen, S. M. Ali, D. E. Oates, R. S. Withers, and J. A. Kong, "Current distribution, resistance, and inductance for superconducting strip transmission lines," *IEEE Trans. Appl. Superconduct.*, vol. 1, pp. 108–115, June 1991.
[41] L. H. Lee, S. M. Ali, and W. G. Lyons, "Full-wave characterization of high-$T_c$ superconducting transmission lines," *IEEE Trans. Appl. Superconduct.*, vol. 2, pp. 49–57, June 1992.
[42] B. Cabon, T. Vu Dinh, and J. Chilo, "Attenuation, phase velocity and current density distribution in high critical temperature superconducting planar transmission lines," *IEEE Trans. Magn.*, vol. 31, pp. 1570–1573, May 1995.
[43] O. G. Vendik and A. Yu. Popov, "Current distribution in the cross section and resistance per unit length of a superconducting microstrip line," *Tech. Phys.*, vol. 38, pp. 535–538, July 1993.
[44] L. Löfgren and O. G. Vendik, "Analytical formulae for attenuation and phase velocity of a high-$T_c$ coplanar transmission lines," in *Proc. 23rd European Microwave Conf.*, Madrid, Spain, Sept. 1993, pp. 644–645.
[45] J. Pearl, "Current distribution in superconducting film carrying quantized fluxoids," *Appl. Phys. Lett.*, vol. 5, pp. 65–66, Jan. 1964.
[46] W. Heinrich, "Full-wave analysis of superconducting coplanar waveguide with finite conductor thickness," in *Proc. 21st European Microwave Conf.*, Stuttgart, Germany, Sept. 1991, pp. 667–672.
[47] I. B. Vendik, S. S. Gevorgian, D. I. Kaparkov, S. A. Gal'chenko, and E. Carlsson, "Critical limitations in low-loss narrow-band HTSC filter design," in *Proc. 24th European Microwave Conf.*, vol. 1, Cannes, France, Sept. 1994, pp. 522–527.
[48] I. B. Vendik, O. G. Vendik, S. S. Gevorgian, M. F. Sitnikova, and E. Olsson, "A CAD model for microstrips on r-cut sapphire substrates," *Int. J. Microwave Millimeter-Wave Computer-Aided Eng.*, vol. 4, pp. 374–383, Oct. 1994.
[49] I. B. Vendik and E. T. Kalendarov, "CAD model of effective dielectric constant of microstrip line on M-cut sapphire substrate," *Int. J. Microwave Millimeter-Wave Computer-Aided Eng.*, vol. 5, pp. 402–405, Nov. 1995.
[50] M. Kirshning, R. H. Jansen, and N. H. L. Koster, "Measurement and computer-aided modeling of microstrip discontinuities by an improved resonator method," *IEEE MTT-S Int. Microwave Symp. Dig.*, Boston, MA, May 1983, pp. 495–497.
[51] A. Deleniv, T. Martinsson, and I. Vendik, "CAD model of high-$T_c$ superconducting coplanar waveguide resonator on isotropic and anisotropic substrate," in *Proc. 26th European Microwave Conf.*, vol. 1, Prague, Czech Republic, Sept. 1996, pp. 510–513.
[52] S. Gevorgian, A. Deleniv, T. Martinsson, S. Gal'chenko, P. Linner, and I. Vendik, "CAD model of a gap in a coplanar waveguide," *Int. J. Microwave Millimeter-Wave Computer-Aided Eng.*, vol. 6, pp. 369–377, Sept. 1996.
[53] I. Vendik, D. Kaparkov, and S. Gevorgian, "High $T_c$ superconductor microstrip resonator on sapphire substrate (r-cut)," in *Proc. 25th. European Microwave Conf.*, vol. 2, Bologna, Italy, Sept. 1995, pp. 1295–1297.

**Orest G. Vendik** (M'92) was born in Leningrad, Russia, in 1932. He received the diploma of radio engineer, candidate of Sc. degree (Ph.D.), and Doctor of Sc. degree from Leningrad Electrical Engineering Institute (now St. Petersburg Electrotechnical University), St. Petersburg, Russia, in 1954, 1957, and 1966, respectively.

In 1964, he joined the Department of Applied Physics, St. Petersburg Electrotechnical University, as a Professor, and is currently with the Electronics Department. From 1967 to 1968, he was a Researcher on leave at Surrey University, London, U.K. From 1969 to 1989, he held the position of Head of the Department of Electron–Ion Technology, where he is currently Professor in the same department, as well as Head of the Cryoelectronics Group. He works periodically as a Visiting Professor at Chalmers University of Technology, Gothenburg, Sweden. His research interests have been in the foundation of solid-state electronics (ferrites, ferroelectrics, superconductors) and microwave physics. His concentration is on properties and applications of HTS's and ferroelectrics at microwaves. He takes part in elaboration of microwave components based on S–N (superconducting–normal) transition and voltage-controlled ferroelectrics: signal limiters, switches, and phase shifters.

Dr. Vendick is a member of the St. Petersburg Association of Scientists, St. Petersburg, Russia.

**Irina B. Vendik** (M'96) received the electronics engineer diploma, and candidate of Sc. (Ph.D.) degree from Leningrad Electrical Engineering Institute (now St. Petersburg Electrotechnical University), St. Petersburg, Russia, in 1959 and 1964, respectively, and the D.Sc. (Phys.) degree from A. F. Ioffe Physicotechnical Institute, St. Petersburg, Russia, in 1990.

She is currently a Professor in the Department of Microelectronics and Radio Engineering, and the Head of the Microwave CAD Group, St. Petersburg Electrotechnical University. She works periodically as a Visiting Professor at Chalmers University of Technology, Gothenburg, Sweden. Her general research interests have been in foundations of solid-state physics and microwave electronics: low-dimensional crystals at microwaves, p-i-n diode switches and phase shifters, and microwave applications of HTS's. Her current activity is in the area of elaboration of HTS microwave components: resonators, filters, power dividers, switches, and phase shifters. She is also interested in a development of CAD-oriented models of HTS planar components in linear and nonlinear approach.

**Dimitri I. Kaparkov** was born in Leningrad, Russia, in 1961. He received the diploma of radio engineer, and candidate of Sc. degree (Ph.D.) from Leningrad Electrotechnical Institute (now St. Petersburg Electrotechnical University), St. Petersburg, Russia, in 1984 and 1997, respectively.

In 1984, he joined the Microwave Research Group, Department of Microelectronics, St. Petersburg Electrotechnical University. His main research interests are in the field of applications of high-temperature superconductors at microwaves, including modeling and CAD development. He is a regular participant in European microwave conferences and the European Conference on Applied Superconductivity.